Molecular Immunology 111 (2019) 32–42

Contents lists available at ScienceDirect

Molecular Immunology

journal homepage: www.elsevier.com/locate/molimm

PI3K activity in dendritic cells exerts paradoxical effects during autoimmune inflammation

Hannes Datler[a], Andrea Vogel[a,b], Martina Kerndl[a,b], Christina Baumgartinger[a], Laszlo Musiejovsky[a], Nina Makivic[a], Sophie Frech[a], Birgit Niederreiter[c], Thomas Haider[d], Marlene Pühringer[a], Julia Stefanie Brunner[a,b], Omar Sharif[a,b,*,1], Gernot Schabbauer[a,b,*,1]

[a] Institute for Vascular Biology and Thrombosis Research, Center for Physiology and Pharmacology, Medical University of Vienna, Vienna, Austria
[b] Christian Doppler Laboratory for Arginine Metabolism in Rheumatoid Arthritis and Multiple Sclerosis, Vienna, Austria
[c] Division of Rheumatology, Department of Internal Medicine III, Medical University of Vienna, Vienna, Austria
[d] Department of Orthopedics and Trauma Surgery, Medical University of Vienna, Vienna, Austria

ARTICLE INFO

Keywords:
PI3K
p85α regulatory subunit
EAE
T_H1
T_H17
IFN-γ

ABSTRACT

The peripheral activation of autoreactive T cells and subsequent central nervous system (CNS) immune cell infiltration are key events relevant for experimental autoimmune encephalomyelitis (EAE), a commonly employed multiple sclerosis (MS) model, influenced by T_H1 and T_H17 mediated immunity. The phosphoinositide-3-kinase (PI3K)-AKT kinase pathway modulates outcome during EAE, with direct actions of PI3K on adaptive immunity implicated in deleterious and effects on antigen presenting cells involved in beneficial responses during EAE. Here, by genetically deleting the regulatory subunit of Class Ia PI3K, p85α, in selective myeloid cells, we aimed to resolve the impact of PI3K in EAE. While genetically deleting PI3K in LysM expressing cells exerted unremarkable effects, attenuating PI3K function in $CD11c^+$ dendritic cells (DCs), promoted secretion of pathogenic EAE promoting cytokines, particularly skewing T_H1 and T_H17 immunity, while notably, improving health in EAE. Neutralizing IFN-γ activity using blocking antibodies revealed a prolonged T_H1 response was critical for the decreased disease of these animals. Thus, PI3K-AKT signaling in DCs acts in a paradoxical manner. While attenuating EAE associated T_H1 and T_H17 responses, it impairs health during autoimmune inflammation.

1. Introduction

Tolerance is critical for preventing aberrant over-activation of adaptive immune cells towards self-derived antigen and thus restrains autoimmunity. Multiple sclerosis (MS) is a chronic inflammatory central nervous system (CNS) autoimmune disease afflicting over 2 million people worldwide characterized by focal inflammatory lesions, demyelination, gliosis and axonal loss that lead to various clinical symptoms including; sensory/visual disturbances, motor impairments, fatigue, pain and cognitive deficits (Lassmann et al., 2007). Although the exact mechanisms underlying MS pathogenesis are poorly understood, the animal model of experimental autoimmune encephalomyelitis (EAE), resembles many key features of MS and has yielded invaluable insight into the mechanistic aspects of disease (Constantinescu et al., 2011). EAE models have revealed the critical role for the peripheral activation of autoreactive T cells and subsequent

Abbreviations: anti-IFN-γ, functional blocking antibody against IFN-γ; AKT, protein kinase B; APC, professional antigen presenting cell; BM-DC, bone marrow derived dendritic cell; CFA, complete freud's adjuvant; CNS, central nervous system; dLN, inguinal draining lymph node; EAE, experimental autoimmune encephalitis; GM-CSF, granulocyte-macrophage colony-stimulating factor; gp61, lymphocytic choriomeningitis virus peptide (position 61–80); GSK3β, glycogen synthase kinase 3β; H&E, hematoxylin and eosin staining; IFN-γ, Interferony; IL, interleukin; LCMV, lymphocytic choriomeningitis virus; moDC, monocyte derived dendritic cell; MOG_{35-55}, myelin-oligodendrocyte-glycoprotein peptide (position 35–55); moMO, monocyte derived macrophage; MS, multiple sclerosis; OVA, ovalbumin (chicken); p38, MAP-kinase; p85α, regulatory subunit p85α; PAMPs, pathogen associated molecular patterns PI3K: phosphoinositol-3-kinase; PIP_3, phosphoinositol-3-phosphate; PTEN, phosphatase and tensin homolog; PTX, pertussis toxin; RORγT, RAR-related orphan receptor gamma T; TGF-β, transforming growth factor β; T_H, T helper cell; T_H1, effector T helper cell type 1; T_H17, effector T helper cell type 17; T-bet, T-Cell-Specific T-Box Transcription Factor; T-reg, regulatory T helper cell

* Corresponding authors at: Institute for Vascular Biology and Multiple Sclerosis, Center for Physiology and Pharmacology, Medical University of Vienna, Vienna, Austria.
E-mail addresses: omar.sharif@meduniwien.ac.at (O. Sharif), gernot.schabbauer@meduniwien.ac.at (G. Schabbauer).
[1] These authors contributed equally.

https://doi.org/10.1016/j.molimm.2019.03.015
Received 6 February 2019; Received in revised form 21 March 2019; Accepted 30 March 2019
Available online 05 April 2019

CNS immune cell infiltration. Key players include T_H1 and T_H17 skewed $CD4^+$ T cells, $CD8^+$ cells, neutrophils, monocytes and monocyte derived macrophages or dendritic cells that propagate resident microglial activation, ultimately triggering tissue injury (Ajami et al., 2011; Aube et al., 2014; Fletcher et al., 2010; Murphy et al., 2010; Rumble et al., 2015). However, the exact interplay between these cell types and the molecular mechanisms that fine tune effector T cell function remain unclear.

Current findings highlight an importance for infiltrating monocytes as drivers of disease since impairing their C-C chemokine receptor type 2 (CCR2) dependent recruitment prevents progression from very mild to severe disease (Ajami et al., 2011). After transmigration into the CNS, monocytes differentiate into monocyte derived-macrophages or monocyte derived-dendritic cells (moMOs/moDCs) and upregulate a set of cell surface markers including F4/80, CD11c and MHC II (Brendecke and Prinz, 2015; Greter et al., 2005; King et al., 2009). Granulocyte-macrophage colony-stimulating factor (GM-CSF) promotes moDC differentiation (Helft et al., 2015) and during EAE is secreted by autoaggressive T cells, inducing inflammatory responses of $CCR2^+$ monocytes and consequently tissue damage. Indeed, mice lacking the GM-CSF receptor specifically in CCR2 expressing cells including monocytes and their progeny are fully resistant to EAE due to a failure in the accumulation of GM-CSF driven moDCs in lymph nodes that is crucial for pathogenic T cell expansion. Indeed, deletion of the GM-CSF receptor on $CCR2^+$ cells in mice already suffering from the first disease symptoms leads to amelioration of established CNS inflammation, suggesting maintenance of GM-CSF signaling on $CCR2^+$ CNS infiltrating cells is indispensable for pathogenesis (Croxford et al., 2015). Interestingly, GM-CSF produced by $CD4^+$ T cells exerts effects in T_H cells independently of key cytokines involved in EAE, including IL-17 and IFN-γ (Codarri et al., 2011). Nonetheless, multiple studies demonstrate the critical role of these aforementioned cytokines in disease pathogenesis and they are generally associated with detrimental effects in EAE (Ajami et al., 2011; Aube et al., 2014; Fletcher et al., 2010; Murphy et al., 2010; Rumble et al., 2015). Thus, pathways that modulate IL-17 and IFN-γ production along with the accumulation of T_H1 and T_H17 cells or those that promote peripheral tolerance in disease could provide valuable knowledge that might have therapeutic implications for MS.

Phosphoinositide-3-kinase (PI3K)-AKT kinase signaling is critical for cellular function and regulates numerous cell fate decisions including survival, metabolism, proliferation and migration There are four PI3K subclasses; with class IA PI3K, comprising a catalytic subunit (p110α, β, or δ) and a regulatory subunit (p85α, p55α, p50α, p85β, or p55γ). Three genes encode for p85: p85α, p55α, and p50α, are encoded by *pik3r1*, via alternative transcription and p85β and p55γ, are encoded by *pik3r2* and *pik3r3*, respectively. The regulatory subunit of PI3K is essential for the stabilization of the catalytic subunit and for the recruitment of phosphor-tyrosines on adaptor molecules and is therefore critical for PI3K-AKT signaling (Covarrubias et al., 2015; Engelman et al., 2006; Luo et al., 2005).

PI3K-AKT signaling regulates immunity and influences the reactivity of myeloid cells following pathogen-associated molecular pattern (PAMP) challenge by fine-tuning cytokine release (Guha and Mackman, 2002; Luyendyk et al., 2008; Vergadi et al., 2017). We and others demonstrated that myeloid cell specific deletion of the negative regulator of PI3K, Phosphatase and Tensin Homolog (PTEN), induces an anti-inflammatory (M2) macrophage signature (Lu et al., 2017; Sahin et al., 2014). This is associated with better outcome during EAE, indicating sustained PI3K signaling within myeloid cells exerts beneficial effects during disease (Sahin et al., 2014). Further, PTEN deficiency in $CD11c^+$ dendritic cells (DCs) improved disease pathogenesis and these beneficial effects were associated with attenuated IL-23 levels which is critical for T_H17 effector cell generation (McGeachy et al., 2009; Sahin et al., 2015). These data provide support for the concept that augmented PI3K signaling within macrophages and DCs is advantageous in the context of EAE. Paradoxically, others have shown that inhibiting downstream actions of PI3K-AKT signaling by reducing mTOR activity through rapamycin treatment decreases EAE severity and implicated this favorable outcome with impaired T_H17 effector cell differentiation (Kurebayashi et al., 2012). While pharmacological inhibition or genetic deficiency of Class 1B PI3K-γ is dispensable for T_H1 and T_H17 cell differentiation, it significantly ameliorated EAE pathogenesis, by affecting CNS T cell chemotaxis (Berod et al., 2011; Li et al., 2013). Further, mice with catalytically inactive Class 1A PI3K-δ, exhibited better outcome during EAE compared to controls and this was associated with decreased T_H17 cells in the lymph nodes and spinal cords. In line, pharmacological inhibition of PI3K-δ, decreased T_H17 effector cell differentiation through intrinsic defects in T cell activation independent of DC function (Haylock-Jacobs et al., 2011). Together, PI3K-AKT signaling plays an important role in the pathogenesis of EAE and the generation of effector T cell functions, with studies indicating both beneficial and detrimental functions.

Here we crossed p85α *loxP/loxP* mice with LysM-Cre or CD11c-Cre expressing animals to specifically attenuate PI3K signaling in monocytes/macrophages and neutrophils or dendritic cells respectively. Using these tools we aimed to provide further insight into the controversial roles of PI3K-AKT signaling in EAE and effector T cell generation.

2. Methods

2.1. Mice

All animals were bred and housed in a specific pathogen-free facility at the Medical University of Vienna. Floxed p85α mice (*Pik3r1*^{tm1Lcd}/J) (Luo et al., 2005) were crossed with LysMCre (B6.129P2-*Lyz2*$^{tm1(cre)Ifo}$/J) and CD11cCre (B6.Cg-Tg(Itgax-cre)1-1Reiz/J) expressing mice (Jackson Laboratory) to generate $p85a^{f/f}$ΔMO and $p85a^{f/f}$ΔDC mice, respectively. Animals were genotyped with the following primers: *Pik3r1:* 5′-GGT TTC TTA CTT TAG ACG GAG CTG-3′ and 5′-CAG ACA GAC CAA CCT AGA GAT TAG G-3′; Cre recombinase: forward, 5′-TCG CGA TTA TCT TCT ATA TCT TCA G-3′ and 5′-GCT CGA CCA GTT TAG TTA CCC-3′. EAE was induced in 8–12 weeks old female littermates. All animal experiments comply with the institutional guidelines for animal experimentation at the Medical University Vienna and were conducted in strict accordance to European law. An ethical approval (0010-WF/V/3b/2016) was obtained by the Federal Ministry for Science and Research, Vienna, Austria.

2.2. EAE induction, IFN-γ blockage and T cell responses

Active EAE was induced in $p85a^{f/f}$ΔDC, $p85a^{f/f}$ΔMO and wildtype (WT) littermate controls. Immunization was performed by subcutaneous injection of 75 µl of 1 mg/ml MOG_{35-55} (Charite Berlin) in emulsified in 75 µl CFA (F5506-10 × 10ML, Sigma-Aldrich), which was enriched with 10 mg/ml *Mycobacterium tuberculosis* (H37Ra; Difco/BD Pharmingen). A total of 200 ng pertussis toxin from *Bordetella pertussis* (BioTrend) was administered intraperitoneally at days 0 and 2 post-immunization. Clinical signs of EAE were assessed with the following disease scores: 0, no disease; 0.5, starting tail weakness; 1, tail weakness; 1.5, tail weakness and starting paralysis of hind limbs; 2, paraparesis; 2.5, severe paraparesis; 3, paraplegia; 4, paraplegia with forelimb weakness; and 5, moribund or dead animals. EAE experiments were terminated at the indicated stages of disease development. For IFN-γ blockage, 6 days post immunization, mice were injected intraperitoneally with IFN-γ blocking antibody (16-7311-81, clone: XMG1.2; eBioscience) or an according isotype control antibody (400452, clone: RTK2071; BioLegend) at a concentration of 100 µg/kg body weight. Lymphocytes of the inguinal draining lymph nodes were harvested and re-stimulated in vitro with 30 µg/ml MOG_{35-55} peptide for 72 h. Supernatants were used to determine T cell cytokine

production.

2.3. Bone marrow dendritic cell (BM-DC) and macrophage (BM-MO) differentiation and primary peritoneal macrophage isolation

Bone marrow cells were flushed from femurs and tibias. BM-DCs and BM-MOs were generated from isolated cells that were resuspended in complete RPMI medium (10% fetal calf serum, 5% glutamine and 5% Pen/Strep) supplemented with 20 ng/ml recombinant mouse GM-CSF (415-ML-050, R&D Systems) for BM-DC or 40 ng/ml M-CSF (416-ML-050, R&D Systems) for BM-MO generation at 37 °C in a 5% CO_2 atmosphere. After 3 days, cells were replenished with fresh medium supplemented with either respective cytokine. $1*10^6$/ml non-adherent BM-DCs were harvested 6 days post differentiation, re-plated and stimulated with LPS (tlrl-pelps, InvivoGen), and IFN-γ (PMC4031, ThermoFisher) the following day as indicated. In experiments involving p38 inhibition, SB203580 (Adipogen, AG-CR1-0030-M001) was used. After washing two times with PBS, $1*10^6$/ml adherent BM-MOs were harvested and lysed in RIPA buffer (Section 2.6) for western blotting. Peritoneal macrophages were isolated using peritoneal lavage with 7 ml of sterile saline. Lavage fluid was collected in sterile tubes and peritoneal macrophages were collected by centrifugation at 500*g* for 5 min at 4 °C. 1×10^6 cells/ml were lysed in 10 µl RIPA buffer for western blotting.

2.4. Cell isolation from the spinal cord

Mice were euthanized and transcardially perfused with 20 ml PBS. Spinal cords were extracted, weighed, cut into small pieces and digested in 3 ml digestion medium (DMEM; 1 mg/ml Papain, Sigma-Aldrich, P4762; 0.03 mg/ml DNase I, Roche, 11284932001; 0.5 mg/ml Collagenase/Dispase, Sigma-Aldrich, 10269638001). Subsequently, mechanical and enzymatic dissociation was performed by GentleMACS™ Octo Dissociator with Heaters (Miltenyi Biotec) with a brain specific program (37C_ABDK_01). Digestion was stopped by addition of 5 ml of neutralization medium (DMEM, 10% FBS). The brain homogenate was filtered through a pre-wet 40 µm cell strainer and post washing centrifuged at 250*g* for 4 min at RT. The supernatant was discarded, and isolated cells were separated using a 70/37/30% layered Percoll gradient (Sigma-Aldrich, P1644) with centrifugation at 800*g* for 40 min at 18 °C without brake. Subsequently, the layer of debris and myelin was removed and 3 ml of the immune cell containing 70/37% interphase was collected, washed with 9 ml 1xHBSS (Gibco, 14175-05) and pelleted by centrifugation at 500*g* for 4 min at 4 °C. After another washing step with 1 ml 1xHBSS and centrifugation for 7 min, the pellet was resuspended in 500 µl FACS buffer. Finally, cells were counted and further prepared for flow cytometry.

2.5. Mixed lymphocyte reaction in vitro

BM-DCs derived from $p85a^{f/f}\Delta DC$ and wildtype (WT) littermate controls were activated with LPS (100 ng/ml) and OVA peptide (50 µg/ml, H-5532.1000, Bachem). Pulsed BM-DCs were cocultured with MACS-isolated (130-104-454, Miltenyi Biotec, performed according to manufacturer's protocol) $CD4^+$ T cells from OTII mice (B6.Cg-Tg (TcraTcrb)425Cbn/J; The Jackson Laboratory) at a ratio of 1:5. Three days post culture, supernatants were collected for cytokines measurements using ELISA and cells were re-stimulated with Phorbol 12-myristate 13-acetate (500 ng/ml, 79346, Sigma) and Ionomycin (1 µg/ml, I0634, Sigma) for 3 h and processed for intracellular flow cytometry.

2.6. Flow cytometry

Differentiated BM-DCs were filtered through a 40 µm nylon strainer (Corning, Falcon) and stained with following antibodies: CD45.2-BV650 (109836, clone: 104, BioLegend), CD86-FITC (105-005, clone: GL-1, BioLegend), Siglec-F-PE-Cy5.5 (565526, clone: E50-2440, BD Pharmingen), F4/80-AF-700 (123129, clone: BM8, BioLegend), CCR2-BV421 (150605, clone: SA203G11, BioLegend), CX_3CR1-BV510 (149025, clone: SA011F11, BioLegend), MHC II-BV605 (107639, clone: M5/114.15.2, BioLegend), CD3e-PE-Cy-5.5 (TO-65-0031-U025, clone: 145-2C11, TONBO), B220-PE-Cy5.5 (55-0452, clone: RA3-6B2, TONBO) and CD11b-APC (17-0112, clone: M1/70, eBioscience). Post mixed lymphocyte reaction or EAE, intracellular staining in $CD4^+$ T cells was performed by staining cells for the surface markers CD3e-RedFluor 710 (80-0032, clone: 17A2, Tonbo), CD45.2-BV650 (109836, clone: 104, BioLegend), CD4-PerCP-Cy-5.5 (clone GK1.5, 100433, Biolegend) and viability (Fixable Viability Dye eFluor 780, 13539140). Cells were subsequently fixed and permeabilized with the eBioscience™ Intracellular Fixation & Permeabilization Buffer Set according to the manufacturer's instructions. Cells were stained for IL-17-BV605 (506927, clone: TC11-18H10.1, Biolegend) and IFN-γ-PE (12-7311, clone: XMG1.2, eBioscience) respectively. Isotype controls were included for IL-17 (#400161, Biolegend) and IFN-γ (#12-4321-41, eBioscience). Data was acquired using CytoFLEXs (Beckman Coulter, Inc.) and analyzed with CytExpert (Version 2.2.0.97; Beckman Coulter, Inc.) and FlowJo (Version 10, LLC) software.

2.7. Immunoblotting

Cells were harvested and lysed in RIPA buffer (150 mM NaCl; 50 mM Tris pH 7.3; 0.1% SDS; 1% NP-40; 0.5% sodium-deoxycholatate; 1 mM sodium ortho-vanadate pH 10 (pre-activated); 1 mM EDTA). Protein content was determined by Pierce BCA Protein Assay according to the manufacturer's protocol (23225, ThermoFisher). Samples were denatured in 5x Laemmli buffer (300 mM TrisCl pH: 6.8; 60% glycerol; 10% SDS; 0.025% bromphenolblue; 7% β-mercaptoethanol), separated by SDS-PAGE on a 10% denaturing polyacrylamide gel and blotted onto a polyvinylidene difluoride membrane (Millipore), which was blocked for 1 h with 5% dry milk/0.1% Tween20. Membranes were incubated with primary antibodies (all Cell Signaling Technologies) p-AKT (9275S), AKT (C67E7), p-p38 (9211S), p-GSK-3β (9211S) or β-actin (9211S, Sigma) overnight at 4 °C and incubated with the respective HRP-coupled secondary antibody (Anti-Rabbit HRP, 7074, Cell Signaling Technologies) at room temperature for 2 h. Proteins were detected using chemo luminescence (SuperSignal West Femto Maximum, Thermo Fisher) on a FluorChem HD2 chemo luminescence imager (Alpha Innotech). Signal-intensity was quantified by densitometry analysis with Image J software and was normalized to the according control band (β-actin or AKT).

2.8. Organ homogenization

Organs were snap frozen in liquid nitrogen. Samples were homogenized with 20 cycles of 5000 rpm for 15 s (Precellys 24; Bertin Technologies) in Trifast (30-2010, VWR) for RNA isolation, or in Greenberger buffer (150 mM NaCl, 15 mM Tris base, 1 mM $MgClx6H_2O$, 1 mM $CaCl_2x2H_2O$, Tritron 1%, pH to 7.4) for cytokine determination by ELISA.

2.9. RT-PCR

RNA of homogenized organs or BM-DCs were harvested using Trifast reagent following the manufacturer's instructions. Reverse transcription was performed using the High Capacity cDNA Reverse Transcription kit (10400745, Fisher Scientific). RT-PCR was performed using Luna Master Mix (M3003E, New England BioLabs) using a StepOne Real-Time PCR System (Applied Biosystems). Levels of target genes were normalized to HPRT or GAPDH and described as fold induction over unstimulated cells. Target primer: *Hprt*: 5′-CGC AGT CCC AGC GTC GTG-3′ and 5′-CCA TCT CCT TCA TGA CAT CTC GAG-3′; *Ifng*: 5′-TGA GCT CAT TGA ATG CTT GG-3′ and 5′-ACA GCA AGG CGA AAA

AGG AT-3′; *Tbx21*: 5′-TCA ACC AGC ACC AGA CAG AG-3′ and 5′-ATC CTG TAA TGG CTT GTG GG-3′; *Il10*: 5′-AGC TGA AGA CCC TCA GGA TG-3′ and 5′-TGG CCT TGT AGA CAC CTT GG-3′; *Foxp3*: 5′-GCG AAA GTG GCA GAG AGG TA-3′ and 5′-TCC AAG TCT CGT CTG AAG GC-3′; *Il17*: 5′-TGA GCT TCC CAG ATC ACA GA-3′ and 5′-TCC AGA AGG CCC TCA GAC TA-3′; *Rorc*: 5′-CCG CTG AGA GGG CTT CAC-3′ and 5′-TGC AGG AGT AGG CCA CAT TAC A-3′.

2.10. ELISA

ELISAs of IFN-γ (88-7314, Invitrogen), IL-6 (88-7064, Invitrogen), IL-12b (88-7121, Invitrogen) IL-17a (88-7371-77, Invitrogen) and IL-23 (DY1887, R&D Systems) were performed according to the manufacturer's protocol. IL-6, IL-12 and IL-23 were quantified in supernatants of GM-CSF derived BM-DCs as indicated. IFN-γ, and IL-17a were detected in supernatants of re-stimulated splenocytes and lymphocytes of MOG-immunized mice after 3 days in culture.

2.11. Histology and immunohistochemistry

Mice were humanly sacrificed and perfused intra-cardiac with 1xPBS. Isolated brain and spinal cords were fixed in 4% buffered formalin. Fixed tissues were paraffin embedded, cut to 2 µm and stained with Klüver–Barrera (KLB) and H&E using standard procedures. At least three cross sections per animal were used for histological evaluation. The inflammatory index represents the total number of mononuclear infiltrates per cross section. Demyelinated areas are defined as percentage over total area of each cross section in the KLB myelin staining.

2.12. ELISPOT

Twenty-seven days post EAE induction, single-cell suspensions were prepared from spleens. A total of $1*10^5$ cells was seeded in quadruplicates and re-stimulated with 5 µg/ml $MOG_{35–55}$ peptide (Charite Berlin), 1 µg/ml lymphocytic choriomeningitis virus (LCMV) peptide$_{61–80}$ (gp61, AnaSpec) or 5 µg/ml anti-CD3/CD28 Dynabeads (Life Technologies) in 96-well MultiScreenHTS-IP Filter Plates (MSIPS4W10; Millipore) using CTL Test serum-free medium (C.T.L.). IL-17a (3321-2 A, Mabtech) and IFN-γ (3521-2 A, Mabtech) ELISPOTs were performed according to the manufacturer's instructions using a BCIP/NBT Liquid Substrate System (B1911, Sigma-Aldrich).

2.13. Statistics

Statistical analysis was performed using a two-tailed *t*-test for two groups, an ordinary one-way ANOVA followed by Bonferroni's multiple comparisons test for multiple groups and an area under the curve (AUC) followed by a two-tailed *t*-test for curve analysis on Prism 8 software (GraphPad, La Jolla, CA). All data represent biological replicates. Statistical significance is indicated by * $p < 0.05$, ** $p < 0.01$, *** $p < 0.001$, **** $p < 0.001$. All error bars indicate standard error of the mean (SEM).

3. Results

3.1. BM-DC expressed p85α promotes PI3K activity restraining cytokine secretion and antigen presentation

To evaluate the role of p85α in dendritic cells, we crossed floxed *Pik3r1* mice (Luo et al., 2005) with animals expressing the Cre recombinase under the CD11c promoter to generate animals with p85α deficiency in CD11c expressing cells (p85a$^{f/f}$ΔDC mice). Using GM-CSF, we differentiated bone marrow cells into DCs (BM-DCs) as previously described (Helft et al., 2015) and validated deletion efficiency of p85a$^{f/f}$ΔDC cells using Western blotting (Fig. 1A). While in the naïve state, BM-DCs null for p85α exhibited unremarkable differences in AKT signaling compared to controls, upon lipopolysaccharide (LPS) challenge, we observed significantly reduced AKT phosphorylation. This was associated with elevated p38 phosphorylation, while minor effects were observed on GSK3β (Fig. 1B, Fig. S1). Evaluating LPS driven cytokine secretion demonstrated augmented IL-6 and IL-12 levels in p85α null BM-DCs compared to WT (Fig. 1C–D). While LPS treatment did not induce IL-23, LPS/IFN-γ treatment induced IL-23 synthesis with increased secretion occurring in p85a$^{f/f}$ΔDC BM-DCs compared to WT controls (Fig. 1E and data not shown). Given that higher LPS induced p38 phosphorylation in BM-DCs lacking p85α was apparent (Fig. 1B, Fig. S1), and others have implicated suppressed PI3K activity in BM-DCs with enhanced IL-12 that is in turn dependent on elevated p38 (Fukao et al., 2002), we next examined whether the augmented LPS driven cytokine secretion of p85a$^{f/f}$ΔDC cells was associated with p38. We thus treated both genotypes of BM-DCs with LPS in the presence or absence of a pharmacological p38 inhibitor and evaluated cytokine levels using ELISA. Indeed, enhanced p38 activation was causally implicated in augmented LPS driven IL-6 and IL-12 secretion in BM-DCs lacking p85α as this did not occur in the presence of p38 inhibition (Fig. S2). Together, these findings suggest that p85α driven signaling within BM-DCs dampens LPS induced inflammation through skewing of the p38 pathway.

In order to validate these findings and examine potential deregulations in GM-CSF driven DC differentiation upon p85α deletion, we next examined the levels of antigen presentation related molecules including MHC II and CD86. BM-DCs were defined as non-adherent $CD45^+CD3^-B220^-SiglecF^-CX_3CR1^+CD11b^+F4/80^+$ cells (Fig. S3), have previously been shown to express both CD11c and F4/80 and comprise a heterogeneous population associated with different MHC II levels, namely MHC II^{int} and MHC II^{hi} (Helft et al., 2015). While under homeostasis no differences were observed, upon LPS treatment, p85α deficient DCs exhibited less of an MHC II^{int} phenotype and were thus to a greater extent MHC II^{hi} (Fig. 1F–G). In line with the crucial role of MHC II in antigen presentation, opposed to the MHC II^{int}, the MHC II^{hi} population exhibited augmented levels of co-stimulatory CD86. Notably, CD86 expression further increased upon p85α deficiency, suggesting that p85α could restrict antigen presentation within DCs (Fig. 1H and Fig. S4). We thus next loaded both genotypes of DCs with OVA peptide, pulsed them with LPS, cultured them together with $CD4^+$ OVA specific OTII T cells, and collected supernatant after 3 days. We could observe that IFN-γ, and IL-17a levels were significantly higher in $CD4^+$ T cells cultured in the presence of BM-DCs lacking p85α (Fig. 1I). In an identical set up, using flow cytometry, we next performed IFN-γ, and IL-17a intracellular staining in $CD4^+$ T cells. While, no IL-17 positive T cells could be detected, strikingly, OVA specific $CD4^+$ T cells co-cultured with BM-DCs from p85a$^{f/f}$ΔDC animals exhibited augmented intracellular IFN-γ compared to WT controls (Fig. 1J–K). An isotype control corroborated specificity for the intracellular IFN-γ staining (Fig. 1K). We conclude that in GM-CSF derived DCs p85α restrains LPS driven signaling, cytokine secretion and antigen presentation.

3.2. p85α presence in CD11c but not LysM expressing cells worsens autoimmunity

Cytokines including IL-6, IL-23, IL-17 and IFN-γ play critical roles in EAE and their requirement has been convincingly demonstrated using genetically deficient mice (Bettelli et al., 2006; Cua et al., 2003; Krakowski and Owens, 1996; Lees et al., 2008; McGeachy et al., 2009; Mendel et al., 1998; Prinz et al., 2008). Noting that upon LPS or LPS/IFN-γ challenge, p85α deficiency within BM-DCs conferred significantly upregulated levels of IL-6, IL-12 and IL-23 and p85α deficient cells likely present more antigen to T cells, skewing them in an IL-17 dependent manner (Fig. 1C–K), we next hypothesized that animals deficient for p85α in $CD11c^+$ DCs might exhibit worsened outcome in EAE. This hypothesis is concordant with data demonstrating the relevance of

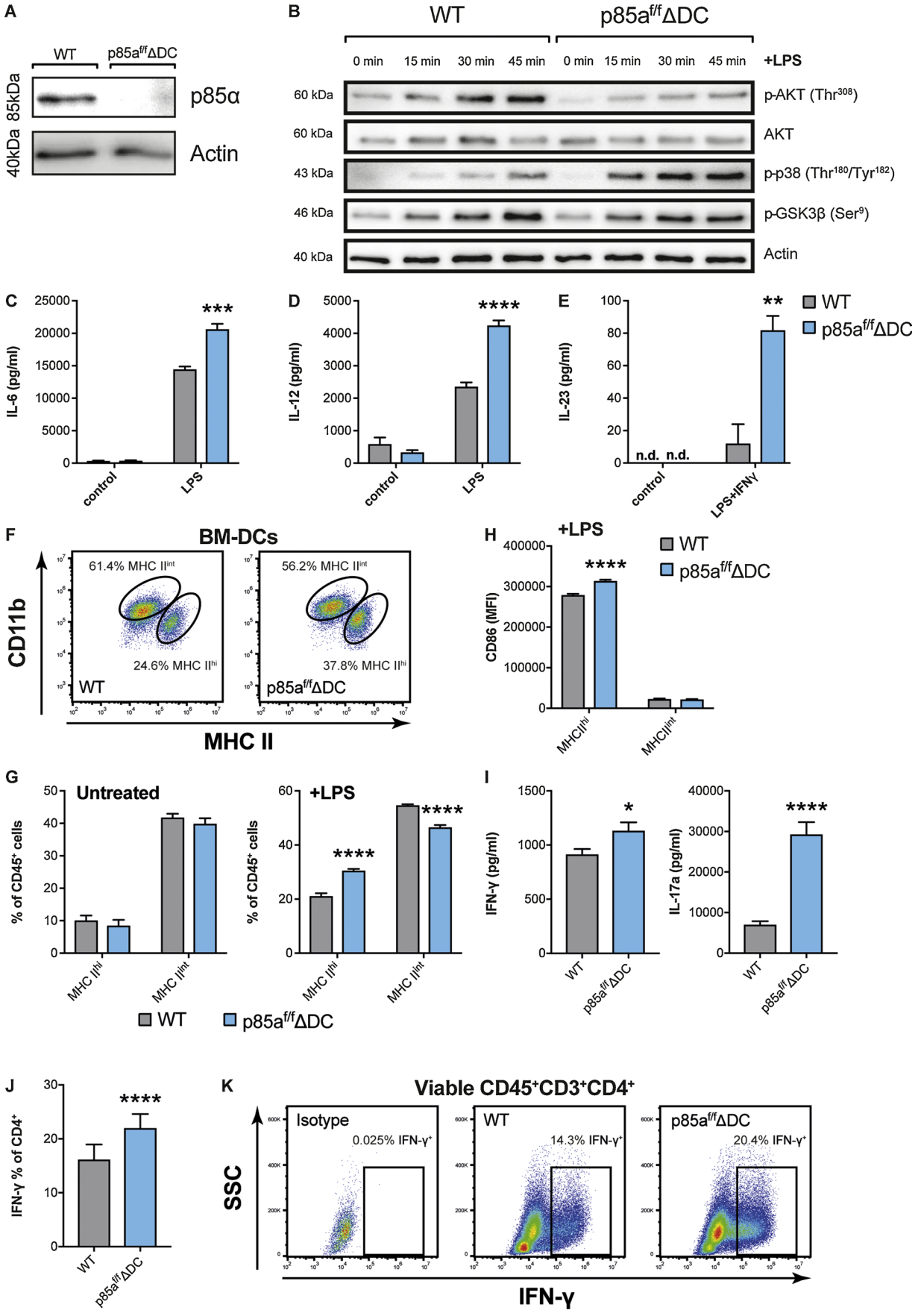

(caption on next page)

Fig. 1. p85α absence lowers PI3K activity, promoting cytokine secretion and antigen presentation. (A) BM-DCs from p85α$^{f/f}$CD11cCre^{+} mice (p85a$^{f/f}$ΔDC mice) and littermate controls were prepared, protein extracted and subsequently blotted for p85α to confirm deletion efficiency. (B) BM-DCs from p85a$^{f/f}$ΔDC mice and littermate controls were stimulated with LPS (10 ng/ml) for 15, 30 and 45 min. Protein extracts were prepared and phosphorylation of AKT, p38 and GSK3β determined by western blotting. (C–D) BM-DCs from both genotypes of mice were prepared and stimulated with LPS (10 ng/ml) for 24 h and IL-6 (C) and IL-12 (D) were determined in the supernatant using ELISA. (E) BM-DCs from both genotypes of mice were stimulated together with LPS (10 ng/ml) and IFN-γ (5 ng/ml) for 24 h and IL-23 levels were determined in the supernatant using ELISA. (F) Representative flow cytometry plots depicting the two populations of MHC II positive cells in BM-DCs from both genotypes 4 h post LPS (100 ng/ml) treatment. (G) Quantification of MHC II^{hi} and MHC II^{int} populations in the naïve state and following 4 h LPS (100 ng/ml) treatment in both genotypes of BM-DCs. (H) Mean fluorescence intensity (MFI) of CD86 expression in populations in (G) post LPS treatment. (I) IFN-γ and IL-17a levels in supernatants of BM-DCs from both genotypes of mice following culture with OTII cells for three days. (*J*) Intracellular IFN-γ staining of OVA-specific CD4^{+} T cells following co-culture with BMDCs from both genotypes of mice post 3 h PMA/Ionomycin (500 ng/ml and 1 μg/ml). (K) Representative dot plots of (*J*) are depicted. Cells were gated on viable CD45^{+}CD3^{+}CD4^{+}. Error bars represent mean ± SEM. n = 4 (C-E); n = 4–5 (G); n = 12 (I); n = 12 (*J*) * p < 0.05, ** p < 0.01, *** p < 0.001, **** p < 0.0001; 2-tailed unpaired Student's *t*-test (C–E, G–J).

GM-CSF responsive moDCs to T_H17 pathogenesis and EAE progression (Croxford et al., 2015; Ko et al., 2014). We thus subjected both genotypes to EAE by subcutaneous immunization with myelin oligodendrocyte glycoprotein (MOG_{35-55}) emulsified in complete freud's adjuvant, enriched with *Mycobacterium tuberculosis* (CFA), injected pertussis (PTX) twice and monitored animals regularly from 3 days post induction, prior to disease onset (Fig. 2A). Clinical scoring revealed animals developed symptoms of disease 14 days post induction and progressively worsened. Strikingly and surprisingly, opposed to WT controls, p85a$^{f/f}$ΔDC animals exhibited highly reduced disease severity as indicated by significantly lower clinical scores associated with absence in weight loss (Fig. 2B). Histology coupled to myelin specific Klüver–Barrera (KLB) staining disclosed that at end point (day 27), there was decreased immune cell infiltration, inflammation and demyelination in spinal cords of p85a$^{f/f}$ΔDC animals opposed to controls, confirming disease protection (Fig. 2C). Together, these findings indicate that p85α dependent promotion of PI3K signaling in CD11c^{+} DCs worsens autoimmunity during EAE. Noting that certain macrophage populations can also express CD11c including resident brain macrophages (Kivisakk et al., 2009; Mrdjen et al., 2018; Mundt et al., 2019), we next set out to examine p85α specificity on immune related effects during EAE. We thus crossed floxed *Pik3r1* mice (Luo et al., 2005) with animals expressing the Cre recombinase under the LysM promoter to generate animals with p85α deficiency in LysM expressing cells (p85a$^{f/f}$ΔMOs). We confirmed the selective deletion of p85α in LysM expressing macrophages opposed to BM-DCs as primary peritoneal macrophages (PMs) from p85a$^{f/f}$ΔMOs but not p85a$^{f/f}$ΔDC animals exhibited substantially decreased protein levels of p85α (Fig. 2D). Deletion efficiency of p85α in LysM expressing cells was also ratified in M-CSF derived bone marrow macrophages (Fig. 2E). Subsequently, we subjected p85a$^{f/f}$ΔMOs and control littermates to EAE in an identical manner to p85a$^{f/f}$ΔDC animals. We could not observe any differences in disease outcome as evaluated using clinical scoring and weight loss (Fig. 2F). Importantly, these data assign a novel and specific role for p85α activity in CD11c expressing cells, likely DCs, in influencing autoimmunity, additionally ruling out significant effects of p85α expression in monocytes, macrophages and neutrophils to disease pathogenesis.

3.3. CD11c expressed p85α dampens EAE associated T_H1 and T_H17 responses

To further evaluate the importance of DC expressed p85α in EAE and corroborate the negligible effects of p85α in macrophages, we next isolated lymph nodes prior to disease onset (day 8) of both groups of animals along with controls, and re-stimulated with MOG_{35-55} peptide. We hypothesized augmented MOG_{35-55} elicited antigen specific responses would occur in p85a$^{f/f}$ΔDC animals versus controls, as p85α deficiency was associated with improved outcome early during disease (Fig. 2B), which was likely linked to a skewed DC antigen presentation ability (Fig. 1F–H). Indeed, elevated IFN-γ and a tendency towards more IL-17a in this experimental set up suggested that p85α deficiency in DCs skewed T cells within the lymph nodes in a T_H1 and T_H17 manner during EAE (Fig. 3A). Confirming the importance of antigen presentation in CD11c expressing cells, no effects were observed in lymph nodes of p85a$^{f/f}$ΔMOs animals, ratifying the unremarkable effects of macrophage expressed p85α in disease. Noting that we only observed tendencies towards elevated IL-17a secretion (Fig. 3A), yet culture of CD4^{+} T cells with p85α deficient BM-DCs clearly primed CD4 responses towards elevated IL-17a (Fig. 1I), we next set out to strengthen the role of p85α deficiency in CD11c^{+} cells on T_H17 driven immunity. In an independent experiment we first isolated splenocytes from EAE suffering mice and could confirm elevated MOG_{35-55} elicited T_H1 and T_H17 responses in spleens of p85a$^{f/f}$ΔDC animals versus controls (Fig. 3B). Evaluating levels of infiltrated spinal cord associated IL-17^{+} CD4^{+} T cells in these identical animals using intracellular flow cytometry revealed that although there was a moderate tendency towards more T_H17 cells in the spines of p85a$^{f/f}$ΔDC animals (p = 0.089), the ability of DC expressed p85α to skew antigen specific responses was clearly more pronounced in secondary lymphoid organs such as the spleen and lymph nodes (Fig. 3A–C). To further corroborate the strong effect of p85α in skewing antigen specific responses in the periphery during EAE, we next cultured splenocytes from EAE-induced p85a$^{f/f}$ΔDC animals versus controls and subjected them to highly sensitive ELISPOT analysis post stimulation with MOG_{35-55} peptide or T cell crosslinking with anti-CD3/CD28. As a control, we stimulated cells with lymphocytic choriomeningitis virus (LCMV) specific gp61 peptide. While gp61 elicited no immune response, strikingly, upon MOG_{35-55} rechallenge or T cell cross-linking, higher levels of both IFN-γ and IL-17a were observed, confirming that T cells were indeed skewed in a T_H1 and T_H17 manner (Fig. 3D–E). We conclude that p85α expression in CD11c expressing DCs promotes peripheral CD4^{+} T cell tolerance to myelin derived antigen by hindering effector T cell activation. Surprisingly, this is associated with worsened outcome during EAE.

3.4. IFN-γ is critical for the detrimental effects of p85α in CD11c + cells during autoimmunity

To further characterize the fate of autoreactive effector T cells upon p85α deficiency in DCs, EAE bearing mice were sacrificed in the progressive disease phase (day 15) and cytokine levels assessed in the lymph nodes. In line to disease onset (Fig. 3A), absolute lymph node IFN-γ levels were elevated in p85a$^{f/f}$ΔDC animals versus controls, a finding confirmed using RT-PCR (Fig. 4A). This was associated with increased expression of the T_H1 defining transcription factor T-bet, corroborating the idea that CD11c associated p85α activity curbed T_H1 responses (Fig. 4B). Evaluating IL-17a levels using RT-PCR confirmed our previous data (Fig. 3), yet we could not observe significant increases in the T_H17 defining transcription factor, RORγT (Fig. 4C). Together, these findings largely support the hypothesis that p85α expression in CD11c^{+} DCs dampens peripheral tolerance during EAE, suggesting its absence is particularly associated with a prolonged T_H1 effector T cell phenotype. Noting that p85a$^{f/f}$ΔDC mice exhibited improved outcome during disease progression (Fig. 2B), we next set out to examine how CD11c expressed p85α in the periphery impacted brain specific immunity. Although protein levels of IFN-γ levels were barely

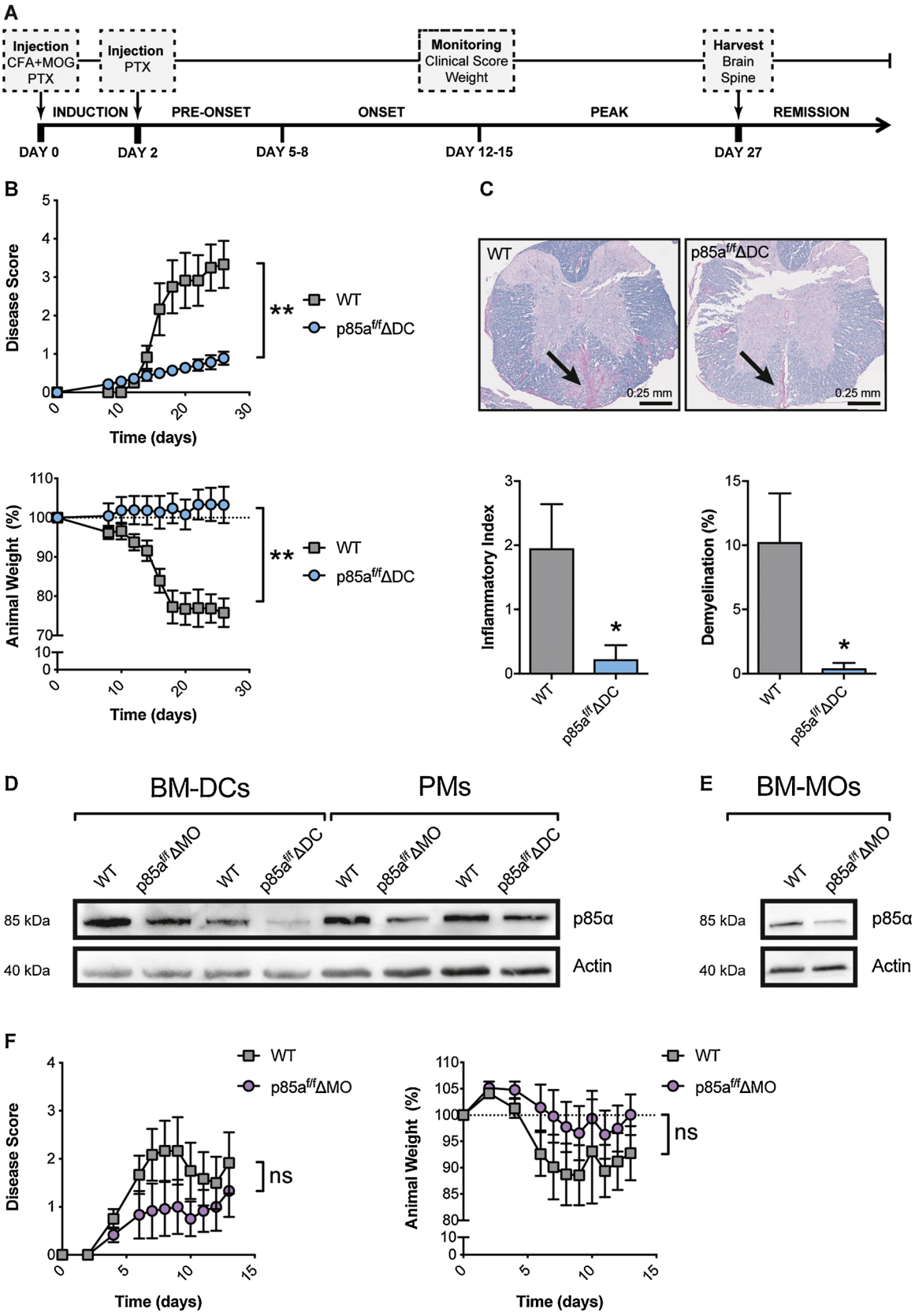

Fig. 2. Specific deficiency of p85α in CD11c expressing cells ameliorates murine EAE progression. (A) Scheme depicting the experimental approach and timeline of murine EAE. (B) Clinical scores and weights of p85a$^{f/f}$ΔDC mice and wildtype littermate controls post EAE. (C) Histology and associated inflammation and demyelination scores of p85a$^{f/f}$ΔDC and control animals 27 days post EAE. (D) BM-DCs and PMs from p85a$^{f/f}$ΔDC, p85a$^{f/f}$ΔMO mice and respective littermate controls were prepared, protein extracted and subsequently blotted for p85α to confirm deletion efficiency. (E) BM-MOs from p85a$^{f/f}$ΔMO mice and littermate controls were prepared, protein extracted and subsequently blotted for p85α to confirm deletion efficiency. (F) Clinical scores and weights of p85a$^{f/f}$ΔMO mice and wildtype littermate controls post EAE. Error bars represent mean ± SEM. n = 6–7 (B); n = 5–6 (C); n = 6 (F) * $p < 0.05$, ** $p < 0.01$; 2-tailed unpaired Student's *t*-test post area under the curve (AUC) (B,F); 2-tailed unpaired Student's *t*-test (C). CFA: Complete Freud's Adjuvant; MOG: Myelin Oligodendrocyte Glycoprotein; PTX: Pertussis

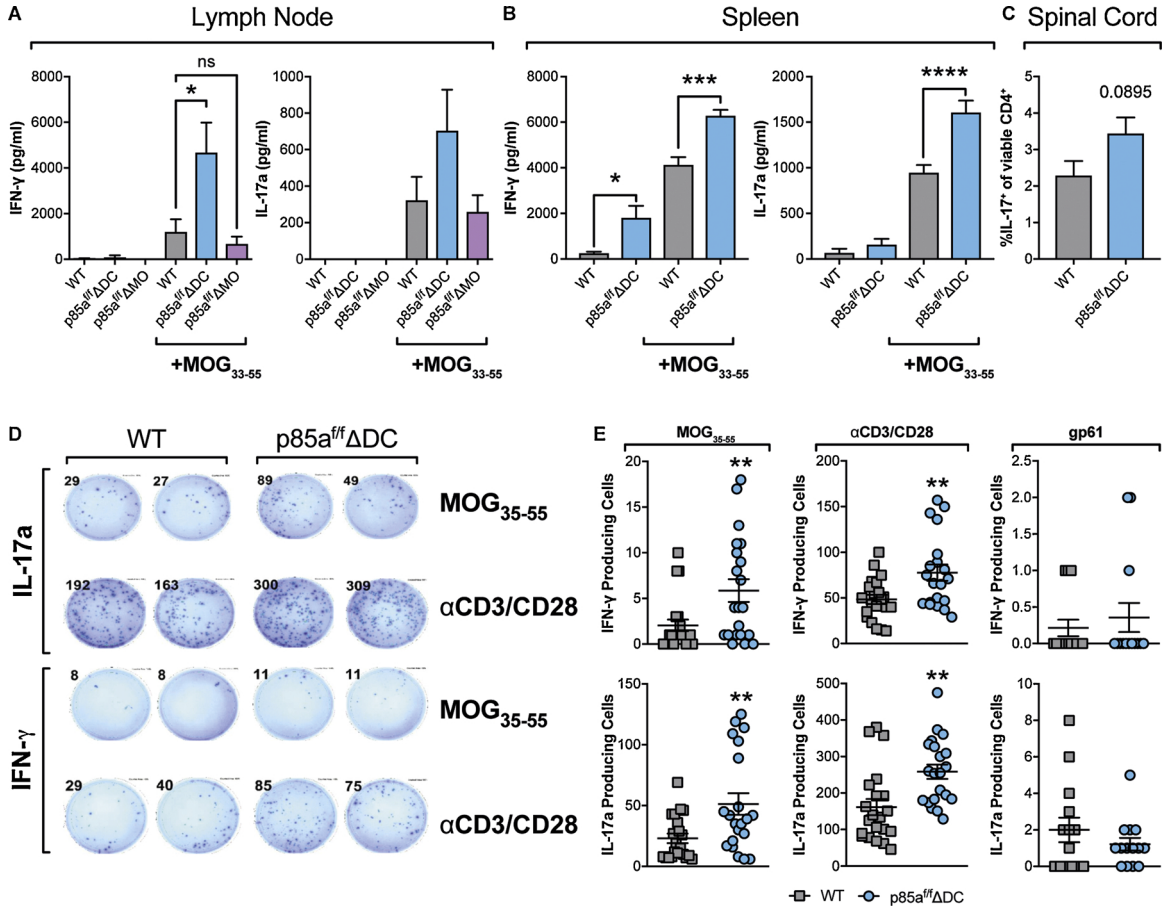

Fig. 3. T cells of p85a$^{f/f}$ΔDC mice exhibit enhanced T_H1/T_H17 polarization in EAE. (A) Draining lymph nodes of p85a$^{f/f}$ΔDC, p85a$^{f/f}$ΔMO and wildtype controls were harvested 8 days post EAE induction. Cells were re-stimulated with MOG_{35-55} (30 μg/ml) for 72 h and IFN-γ and IL-17a secretion detected via ELISA. (B,C) Splenocytes (B) or spinal cords (C) of p85a$^{f/f}$ΔDC and wildtype controls were harvested 8 days post EAE induction. Splenocytes were re-stimulated with MOG_{35-55} (30 μg/ml) for 72 h and IFN-γ and IL-17a secretion detected via ELISA. Spinal cord associated cells were re-stimulated with PMA/Ionomycin (500 ng/ml and 1 μg/ml) for 3 h and intracellularly stained for IL-17. Cells were gated on viable $CD45^+CD3^+CD4^+$. (D–E) IL-17a and IFN-γ ELISPOTs of splenocytes harvested from animals 27 days post EAE induction, stimulated with anti-CD3/CD28 dynabeads (5 μg/ml), MOG_{35-55} (30 μg/ml) and gp61 (1 μg/ml). Representative ELISPOT pictures of IL-17a- and IFN-γ-secreting cells (D) and quantification (E). Error bars represent mean ± SEM. n = 5–7 (A); n = 21 for anti-CD3/28 and MOG_{35-55}; n = 12 (B); n = 5–6 (C); n = 14 for gp61 (*E*); * $p < 0.05$, ** $p < 0.01$, *** $p < 0.001$, **** $p < 0.0001$; One-Way ANOVA (A,B); 2-tailed unpaired Student's *t*-test (C,E).

detectable in the brain using ELISA, RT-PCR of IFN-γ and T-bet suggested that p85α deficiency in $CD11c^+$ DCs likely exerted no impact on brain T_H1 immunity (Fig. 4D and data not shown). This suggested possible impacts of p85α deficiency in $CD11c^+$ DCs on organ specific effector T cell responses. We observed no differences in IL-17a, but interestingly found enhanced RORγT expression (Fig. 4E). As RORγT can control T-reg responses (Gagliani et al., 2015; Lochner et al., 2008), we next evaluated brain expressed IL-10 and Foxp3 levels. Intriguingly, but yet in line with improved outcome of p85a$^{f/f}$ΔDC animals in EAE, we observed higher expression of these T-reg associated molecules in brains of animals deficient for p85α during the progressive disease phase (Fig. 4F). Given our data indicated p85α absence in $CD11c^+$ DCs is strongly associated with an elevated and prolonged peripheral T_H1 effector T cell response that starts at disease onset and remains augmented through-out disease (Figs. 3 and 4), we next elaborated on the potential functional consequences of this. We thus injected animals with IFN-γ blocking or an isotype control antibody, early in EAE, at a time when effector T cell responses are predominant (day 6). Strikingly, blockage of IFN-γ signaling at this early stage significantly dampened the protective phenotype of p85a$^{f/f}$ΔDC animals (Fig. 4G–H). Together, p85α limits peripheral $CD11c^+$ DC T_H1 effector responses in EAE by skewing immunity in an IFN-γ dependent manner which is crucial for the detrimental effects of p85α in $CD11c^+$ cells during autoimmunity.

4. Discussion

The functions of PI3K during EAE remain enigmatic with literature clearly indicating opposing outcomes associated with different effects on adaptive immunity that are likely explained by the distinct experimental approaches employed. Inhibiting PI3Kγ or PI3Kδ pharmacologically or genetically improves EAE outcome and this can be possibly attributed to actions of PI3K on T cell function, including chemotaxis and apoptosis (Berod et al., 2011; Haylock-Jacobs et al., 2011; Li et al., 2013). Modulating adaptive immunity by enhancing PI3K activity in DCs or macrophages through genetic deletion of PTEN also improves EAE outcome (McGeachy et al., 2009; Sahin et al., 2015). Despite the different approaches utilized, the aforementioned studies suggest that direct effects of PI3K on adaptive immunity are deleterious, while PI3K actions on antigen presenting cells are beneficial during EAE. Here, by conditionally genetically deleting the regulatory p85α subunit in selective myeloid cells, we sought to clarify the role of PI3K-AKT signaling in EAE.

Consistent with previous data examining global genetic deletion of p85α, we demonstrate that conditionally targeting p85α in $CD11c^+$ DCs leads to attenuated LPS induced downstream AKT signaling, but increased p38 activation that is associated with augmented IL-12 levels (Fukao et al., 2002). Indeed, pharmacological p38 inhibition is reported

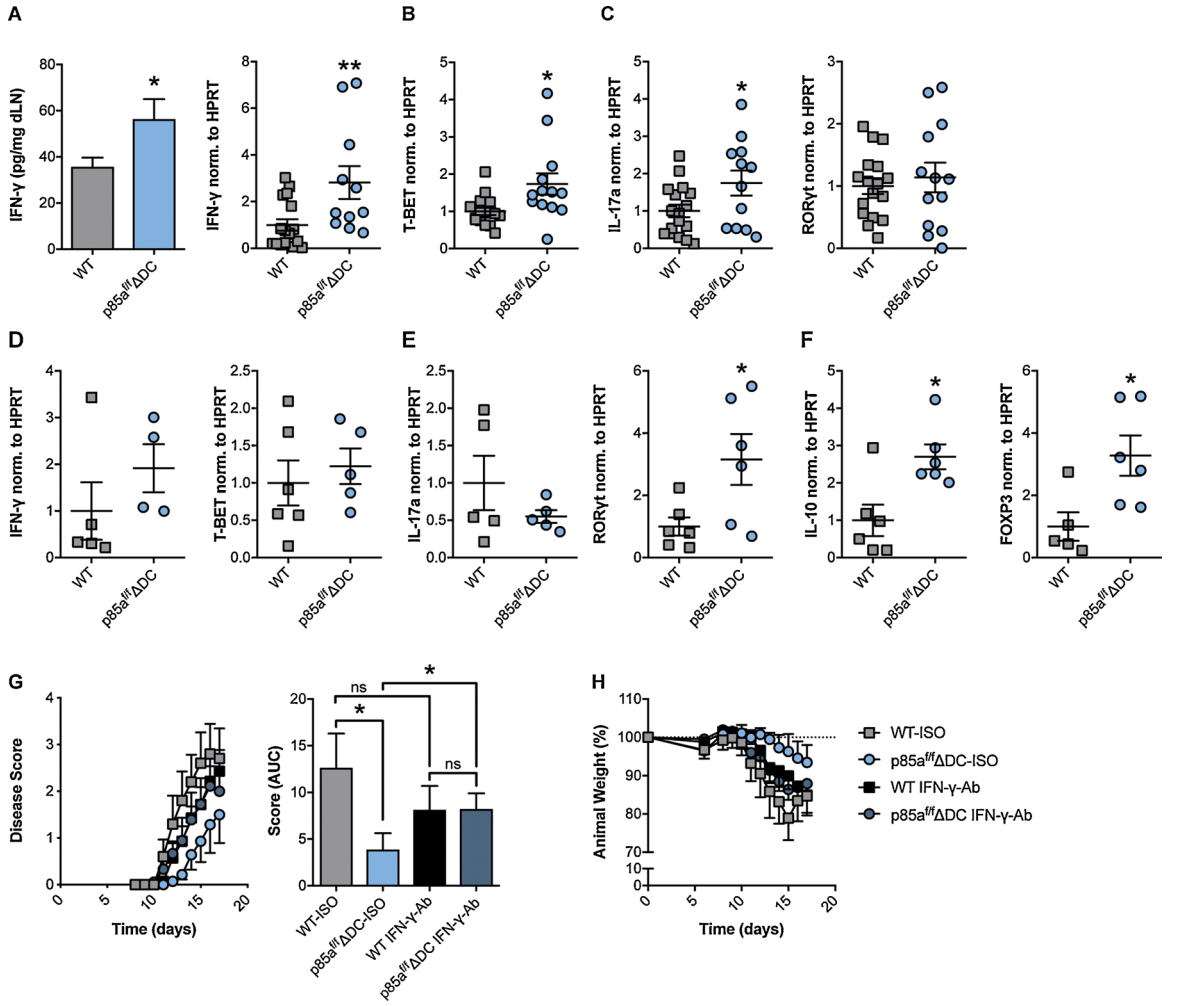

Fig. 4. p85α absence in CD11c$^+$ DCs augments T_H1 effector responses, improving EAE outcome via IFN-γ. (A–C) Draining lymph nodes of p85a$^{f/f}$ΔDC and WT littermate controls were harvested 15 days post EAE. Total IFN-γ was measured in lymph nodes via ELISA (A: left). Cytokine and transcription factor expression was assessed in lymph nodes via RT-PCR (A: right, B–C). (D–F) Brains of p85a$^{f/f}$ΔDC and WT littermate controls were harvested 15 days post EAE and cytokine and transcription factor expression measured via RT-PCR. (G–H) Both genotypes of animals were treated with IFN-γ blocking antibody (IFN-γ-Ab) or isotype control antibody (ISO) and subsequently EAE induced. Error bars represent mean ± SEM. n = 11–17 (A–C); n = 4–6 (D–F), n = 5–8 (G–H); * $p < 0.05$, ** $p < 0.01$; 2-tailed unpaired Student's *t*-test (A–F). 2-tailed unpaired Student's *t*-test post area under the curve (AUC) (G).

to reverse p85α mediated IL-12 increases, which importantly are associated with prolonged T_H1 responses as illustrated by increased resistance of p85α$^{-/-}$ mice opposed to controls following challenge with *Leishmania major*, a parasitic infection in which an adequate T_H1 response is required for controlling disease (Fukao et al., 2002). Aside from augmented IL-12 levels, we demonstrate that p85α null DCs exhibit increased LPS or LPS/IFN-γ triggered IL-6 and IL-23 versus controls. IL-6 exerts detrimental functions in EAE. Compared to controls, IL-6 deficient mice are reported to exhibit reduced CNS inflammation, an effect restored by exogenous IL-6 administration (Mendel et al., 1998). Multiple studies have demonstrated that IL-23 drives EAE pathogenesis. IL-23 signaling is critical for IL-17 production, T_H17 effector cell development and in EAE, IL-23 deficient or IL-23 receptor deficient mice display improved health versus controls (Cua et al., 2003; Langrish et al., 2005; McGeachy et al., 2009). Thus it seems logical that elevated DC derived IL-23, IL-6 and IL-12, along with increased CD86 and MHC II within p85α deficient DCs would lead to a worsened outcome in p85a$^{f/f}$ΔDC animals, presumably associated with augmented IL-17. Surprisingly, this is not the case. In fact, we provide convincing evidence that compared to controls, p85a$^{f/f}$ΔDC animals actually exhibit improved health that is associated with more IL-17 and IFN-γ. Augmented T_H1 and T_H17 responses of antigen specific CD4$^+$ T cells cultured in the presence of BM-DCs lacking p85α contrast those of T cell expressed p85α where it is reported that compared to WT CD4$^+$ T cells, p85α$^{-/-}$ CD4$^+$ T cells produce less IL-17. These differences can possibly be attributed to direct actions of T cell expressed p85α on downstream mTORC1 activation which enhances the nuclear translocation of RORγT promoting T_H17 differentiation (Kurebayashi et al., 2012). Our study demonstrates the paradoxical character of PI3K-AKT signaling in DCs during EAE. Despite dampening EAE associated T_H1 and T_H17 responses, PI3K signaling in DCs is associated with impaired clinical outcome.

IFN-γ is critical for the detrimental effects of DC expressed p85α on health as blocking IFN-γ reversed the beneficial outcome of p85a$^{f/f}$ΔDC animals in EAE. As mentioned earlier, IL-12 increases are associated with prolonged T_H1 responses that are protective during *Leishmania major* infection (Fukao et al., 2002). IL-12 is a heterodimeric molecule composed of p35 and p40 subunits, the latter of which is shared with IL-23, that additionally consists of a p19 subunit (Parham et al., 2002). IL-12 and not IL-23 is required for the development of MOG-specific T_H1 cells since versus controls decreased IFN-γ occurs post MOG re-stimulation of lymph nodes of MOG immunized p35 but not p19 deficient animals (Cua et al., 2003). Given at all EAE stages examined, opposed to controls, we observed more IFN-γ in p85a$^{f/f}$ΔDC mice, we postulate a

prolonged T_H1 response is critical for the improved health of these animals, a proposition concordant with our IFN-γ blocking experiments.

Herein, it is noteworthy that IFN-γ exerts "two-faces" in EAE. Studies utilizing either T-bet deficient mice or transfer of pathogenic IFN-γ^+ T_H1 cells indicate that T-bet deficient mice are protected in EAE and transfer of T_H1 cells elicits EAE, suggesting a pathological role for IFN-γ in disease (Bettelli et al., 2004; Pettinelli and McFarlin, 1981). Conversely, a protective function of IFN-γ in disease has been suggested. Mice lacking IFN-γ are susceptible to EAE and exhibit higher mortality compared to controls suggesting IFN-γ production is not a prerequisite for disease induction and that in fact it exerts disease limiting effects (Ferber et al., 1996; Wang et al., 2006). Experiments with IFN-γ receptor deficient mice also suggest that IFN-γ is dispensable for the generation of MOG specific effector T cells but that it down-regulates the effector and induction disease phases (Willenborg et al., 1996). Later studies demonstrated that IFN-γ inhibits the development of T_H17 cells and promotes the generation of T-regs (Harrington et al., 2005; Wang et al., 2006). Indeed, IFN-γ treatment of $CD4^+CD25-$ T cells causes their conversion into $CD4^+$ T-regs, as demonstrated by increased regulatory function, Foxp3 expression and their ability to suppress EAE upon adoptive transfer (Wang et al., 2006). Given that we observed a prolonged T_H1 response in $p85a^{f/f}\Delta DC$ animals during EAE, it is plausible that this disrupts the initial proliferation of brain specific T_H17 cells leading to their conversion to T-regs. This might explain the higher levels of Foxp3 and IL-10 within the brains of $p85a^{f/f}\Delta DC$ animals versus controls during the progressive disease phase (Fig. 4F), although we cannot rule out that this phenotype simply represents the fact that these animals exhibit improved health at this time (Fig. 2B).

Our data indicate exaggerated MOG specific T_H1 responses occur post MOG re-stimulation of lymph nodes of MOG immunized $p85a^{f/f}\Delta DC$ but not $p85a^{f/f}\Delta MOs$ animals, indicating a specific role for p85α in $CD11c^+$ cells, likely DCs, versus macrophages, monocytes or neutrophils. In this regard, we show that GM-CSF driven BM-DC differentiation of $p85a^{f/f}\Delta DC$ animals primes DCs towards elevated antigen presentation capabilities versus controls, as illustrated by enhanced MHC II and CD86. These data are in contrast to observations in human monocyte derived DCs where pharmacological inhibition of PI3K was associated with lower CD86 levels, DC differentiation and a suppression of T_H1 and T_H17 polarizing cytokines (Xue et al., 2014). These differences could be explained by the distinct experimental approaches employed such as the cell types studied. Our findings also contrast data showing that p85α exerts no effects on DC development or the ability of DCs to activate naïve T cells, although this conclusion related to work that examined splenic DCs from $p85\alpha^{-/-}$ mice (Fukao et al., 2002). While here, we did not examine splenic DCs or other DC subsets, the aforementioned study, together with our data indicates that p85α might exert specific effects on GM-CSF derived moDCs. Mice deficient for the GM-CSF receptor are fully resistant to EAE due to decreased accumulation of GM-CSF driven moDCs in lymph nodes that are crucial for pathogenic T cell expansion (Croxford et al., 2015). Thus p85α driven signaling might be particularly relevant for moDC responses during EAE. Regardless, this study suggests akin to the "two faces" of IFN-γ in EAE, PI3K-AKT signaling in DCs acts as a "double-edged" sword. While attenuating EAE associated T_H1 and T_H17 responses, it impairs clinical outcome. Future work should shed further insight into the paradoxical nature of PI3K-AKT signaling in DCs during EAE.

Funding

This work was supported by funds from the Christian Doppler Laboratory for Arginine Metabolism in Rheumatoid Arthritis and Multiple Sclerosis (to GS) and from the Austrian Science Fund (FWF P30026 to GS and FWF25801-B22 and FWF P31568 to OS). The funders had no role in study design, data collection and analysis, decision to publish, or preparation of the manuscript.

Conflicts of interests

The authors declare that they have no conflicts of interest concerning this article.

Appendix A. Supplementary data

Supplementary material related to this article can be found, in the online version, at doi:https://doi.org/10.1016/j.molimm.2019.03.015.

References

Ajami, B., Bennett, J.L., Krieger, C., McNagny, K.M., Rossi, F.M., 2011. Infiltrating monocytes trigger EAE progression, but do not contribute to the resident microglia pool. Nat. Neurosci. 14, 1142–1149.
Aube, B., Levesque, S.A., Pare, A., Chamma, E., Kebir, H., Gorina, R., Lecuyer, M.A., Alvarez, J.I., De Koninck, Y., Engelhardt, B., Prat, A., Cote, D., Lacroix, S., 2014. Neutrophils mediate blood-spinal cord barrier disruption in demyelinating neuroinflammatory diseases. J. Immunol. Baltimore, Md. 1950 (193), 2438–2454.
Berod, L., Heinemann, C., Heink, S., Escher, A., Stadelmann, C., Drube, S., Wetzker, R., Norgauer, J., Kamradt, T., 2011. PI3Kgamma deficiency delays the onset of experimental autoimmune encephalomyelitis and ameliorates its clinical outcome. Eur. J. Immunol. 41, 833–844.
Bettelli, E., Sullivan, B., Szabo, S.J., Sobel, R.A., Glimcher, L.H., Kuchroo, V.K., 2004. Loss of T-bet, but not STAT1, prevents the development of experimental autoimmune encephalomyelitis. J. Exp. Med. 200, 79–87.
Bettelli, E., Carrier, Y., Gao, W., Korn, T., Strom, T.B., Oukka, M., Weiner, H.L., Kuchroo, V.K., 2006. Reciprocal developmental pathways for the generation of pathogenic effector TH17 and regulatory T cells. Nature 441, 235–238.
Brendecke, S.M., Prinz, M., 2015. Do not judge a cell by its cover–diversity of CNS resident, adjoining and infiltrating myeloid cells in inflammation. Semin. Immunopathol. 37, 591–605.
Codarri, L., Gyulveszi, G., Tosevski, V., Hesske, L., Fontana, A., Magnenat, L., Suter, T., Becher, B., 2011. RORgammat drives production of the cytokine GM-CSF in helper T cells, which is essential for the effector phase of autoimmune neuroinflammation. Nat. Immunol. 12, 560–567.
Constantinescu, C.S., Farooqi, N., O'Brien, K., Gran, B., 2011. Experimental autoimmune encephalomyelitis (EAE) as a model for multiple sclerosis (MS). Br. J. Pharmacol. 164, 1079–1106.
Covarrubias, A.J., Aksoylar, H.I., Horng, T., 2015. Control of macrophage metabolism and activation by mTOR and Akt signaling. Semin. Immunol. 27, 286–296.
Croxford, A.L., Lanzinger, M., Hartmann, F.J., Schreiner, B., Mair, F., Pelczar, P., Clausen, B.E., Jung, S., Greter, M., Becher, B., 2015. The cytokine GM-CSF drives the inflammatory signature of CCR2+ monocytes and licenses autoimmunity. Immunity 43, 502–514.
Cua, D.J., Sherlock, J., Chen, Y., Murphy, C.A., Joyce, B., Seymour, B., Lucian, L., To, W., Kwan, S., Churakova, T., Zurawski, S., Wiekowski, M., Lira, S.A., Gorman, D., Kastelein, R.A., Sedgwick, J.D., 2003. Interleukin-23 rather than interleukin-12 is the critical cytokine for autoimmune inflammation of the brain. Nature 421, 744–748.
Engelman, J.A., Luo, J., Cantley, L.C., 2006. The evolution of phosphatidylinositol 3-kinases as regulators of growth and metabolism. Nat. Rev. Genet. 7, 606–619.
Ferber, I.A., Brocke, S., Taylor-Edwards, C., Ridgway, W., Dinisco, C., Steinman, L., Dalton, D., Fathman, C.G., 1996. Mice with a disrupted IFN-gamma gene are susceptible to the induction of experimental autoimmune encephalomyelitis (EAE). J. Immunol. 1950 (156), 5–7.
Fletcher, J.M., Lalor, S.J., Sweeney, C.M., Tubridy, N., Mills, K.H.G., 2010. T cells in multiple sclerosis and experimental autoimmune encephalomyelitis. Clin. Exp. Immunol. 162, 1–11.
Fukao, T., Tanabe, M., Terauchi, Y., Ota, T., Matsuda, S., Asano, T., Kadowaki, T., Takeuchi, T., Koyasu, S., 2002. PI3K-mediated negative feedback regulation of IL-12 production in DCs. Nat. Immunol. 3, 875–881.
Gagliani, N., Amezcua Vesely, M.C., Iseppon, A., Brockmann, L., Xu, H., Palm, N.W., de Zoete, M.R., Licona-Limon, P., Paiva, R.S., Ching, T., Weaver, C., Zi, X., Pan, X., Fan, R., Garmire, L.X., Cotton, M.J., Drier, Y., Bernstein, B., Geginat, J., Stockinger, B., Esplugues, E., Huber, S., Flavell, R.A., 2015. Th17 cells transdifferentiate into regulatory T cells during resolution of inflammation. Nature 523, 221–225.
Greter, M., Heppner, F.L., Lemos, M.P., Odermatt, B.M., Goebels, N., Laufer, T., Noelle, R.J., Becher, B., 2005. Dendritic cells permit immune invasion of the CNS in an animal model of multiple sclerosis. Nat. Med. 11, 328–334.
Guha, M., Mackman, N., 2002. The phosphatidylinositol 3-kinase-Akt pathway limits lipopolysaccharide activation of signaling pathways and expression of inflammatory mediators in human monocytic cells. J. Biol. Chem. 277, 32124–32132.
Harrington, L.E., Hatton, R.D., Mangan, P.R., Turner, H., Murphy, T.L., Murphy, K.M., Weaver, C.T., 2005. Interleukin 17-producing CD4+ effector T cells develop via a lineage distinct from the T helper type 1 and 2 lineages. Nat. Immunol. 6, 1123–1132.
Haylock-Jacobs, S., Comerford, I., Bunting, M., Kara, E., Townley, S., Klingler-Hoffmann, M., Vanhaesebroeck, B., Puri, K.D., McColl, S.R., 2011. PI3Kdelta drives the pathogenesis of experimental autoimmune encephalomyelitis by inhibiting effector T cell apoptosis and promoting Th17 differentiation. J. Autoimmun. 36, 278–287.
Helft, J., Bottcher, J., Chakravarty, P., Zelenay, S., Huotari, J., Schraml, B.U., Goubau, D., Reis e Sousa, C., 2015. GM-CSF mouse bone marrow cultures comprise a heterogeneous population of CD11c(+)MHCII(+) macrophages and dendritic cells.

Immunity 42, 1197–1211.
King, I.L., Dickendesher, T.L., Segal, B.M., 2009. Circulating Ly-6C+ myeloid precursors migrate to the CNS and play a pathogenic role during autoimmune demyelinating disease. Blood 113, 3190–3197.
Kivisakk, P., Imitola, J., Rasmussen, S., Elyaman, W., Zhu, B., Ransohoff, R.M., Khoury, S.J., 2009. Localizing central nervous system immune surveillance: meningeal antigen-presenting cells activate T cells during experimental autoimmune encephalomyelitis. Ann. Neurol. 65, 457–469.
Ko, H.J., Brady, J.L., Ryg-Cornejo, V., Hansen, D.S., Vremec, D., Shortman, K., Zhan, Y., Lew, A.M., 2014. GM-CSF-responsive monocyte-derived dendritic cells are pivotal in Th17 pathogenesis. J. Immunol. 1950 (192), 2202–2209.
Krakowski, M., Owens, T., 1996. Interferon-gamma confers resistance to experimental allergic encephalomyelitis. Eur. J. Immunol. 26, 1641–1646.
Kurebayashi, Y., Nagai, S., Ikejiri, A., Ohtani, M., Ichiyama, K., Baba, Y., Yamada, T., Egami, S., Hoshii, T., Hirao, A., Matsuda, S., Koyasu, S., 2012. PI3K-Akt-mTORC1-S6K1/2 axis controls Th17 differentiation by regulating Gfi1 expression and nuclear translocation of RORgamma. Cell Rep. 1, 360–373.
Langrish, C.L., Chen, Y., Blumenschein, W.M., Mattson, J., Basham, B., Sedgwick, J.D., McClanahan, T., Kastelein, R.A., Cua, D.J., 2005. IL-23 drives a pathogenic T cell population that induces autoimmune inflammation. J. Exp. Med. 201, 233–240.
Lassmann, H., Bruck, W., Lucchinetti, C.F., 2007. The immunopathology of multiple sclerosis: an overview. Brain Pathol. (Zurich, Switzerland) 17, 210–218.
Lees, J.R., Golumbek, P.T., Sim, J., Dorsey, D., Russell, J.H., 2008. Regional CNS Responses to IFN-γ Determine Lesion Localization Patterns During EAE Pathogenesis.
Li, H., Park, D., Abdul-Muneer, P.M., Xu, B., Wang, H., Xing, B., Wu, D., Li, S., 2013. PI3Kgamma inhibition alleviates symptoms and increases axon number in experimental autoimmune encephalomyelitis mice. Neuroscience 253, 89–99.
Lochner, M., Peduto, L., Cherrier, M., Sawa, S., Langa, F., Varona, R., Riethmacher, D., Si-Tahar, M., Di Santo, J.P., Eberl, G., 2008. In vivo equilibrium of proinflammatory IL-17+ and regulatory IL-10+ Foxp3+ RORgamma t+ T cells. J. Exp. Med. 205, 1381–1393.
Lu, J., Xie, L., Liu, C., Zhang, Q., Sun, S., 2017. PTEN/PI3k/AKT regulates macrophage polarization in Emphysematous mice. Scand. J. Immunol. 85, 395–405.
Luo, J., McMullen, J.R., Sobkiw, C.L., Zhang, L., Dorfman, A.L., Sherwood, M.C., Logsdon, M.N., Horner, J.W., DePinho, R.A., Izumo, S., Cantley, L.C., 2005. Class IA phosphoinositide 3-kinase regulates heart size and physiological cardiac hypertrophy. Mol. Cell. Biol. 9491–9502.
Luyendyk, J.P., Schabbauer, G.A., Tencati, M., Holscher, T., Pawlinski, R., Mackman, N., 2008. Genetic analysis of the role of the PI3K-Akt pathway in lipopolysaccharide-induced cytokine and tissue factor gene expression in monocytes/macrophages. J. Immunol. Baltimore, Md 1950 (180), 4218–4226.
McGeachy, M.J., Chen, Y., Tato, C.M., Laurence, A., Joyce-Shaikh, B., Blumenschein, W.M., McClanahan, T.K., O'Shea, J.J., Cua, D.J., 2009. The interleukin 23 receptor is essential for the terminal differentiation of interleukin 17-producing effector T helper cells in vivo. Nat. Immunol. 10, 314–324.
Mendel, I., Katz, A., Kozak, N., Ben-Nun, A., Revel, M., 1998. Interleukin-6 functions in autoimmune encephalomyelitis: a study in gene-targeted mice. Eur. J. Immunol. 28, 1727–1737.
Mrdjen, D., Pavlovic, A., Hartmann, F.J., Schreiner, B., Utz, S.G., Leung, B.P., Lelios, I., Heppner, F.L., Kipnis, J., Merkler, D., Greter, M., Becher, B., 2018. High-dimensional single-cell mapping of central nervous system immune cells reveals distinct myeloid subsets in health, aging, and disease. Immunity 48, 599.
Mundt, S., Mrdjen, D., Utz, S.G., Greter, M., Schreiner, B., Becher, B., 2019. Conventional DCs sample and present myelin antigens in the healthy CNS and allow parenchymal T cell entry to initiate neuroinflammation. Sci. Immunol. 4.
Murphy, A.C., Lalor, S.J., Lynch, M.A., Mills, K.H., 2010. Infiltration of Th1 and Th17 cells and activation of microglia in the CNS during the course of experimental autoimmune encephalomyelitis. Brain Behav. Immun. 24, 641–651.
Parham, C., Chirica, M., Timans, J., Vaisberg, E., Travis, M., Cheung, J., Pflanz, S., Zhang, R., Singh, K.P., Vega, F., To, W., Wagner, J., O'Farrell, A.M., McClanahan, T., Zurawski, S., Hannum, C., Gorman, D., Rennick, D.M., Kastelein, R.A., de Waal Malefyt, R., Moore, K.W., 2002. A receptor for the heterodimeric cytokine IL-23 is composed of IL-12Rbeta1 and a novel cytokine receptor subunit, IL-23R. J. Immunol. Baltimore, Md 1950 (168), 5699–5708.
Pettinelli, C.B., McFarlin, D.E., 1981. Adoptive transfer of experimental allergic encephalomyelitis in SJL/J mice after in vitro activation of lymph node cells by myelin basic protein: requirement for Lyt 1+ 2- T lymphocytes. J. Immunol. Baltimore, Md 1950 (127), 1420–1423.
Prinz, M., Schmidt, H., Mildner, A., Knobeloch, K.P., Hanisch, U.K., Raasch, J., Merkler, D., Detje, C., Gutcher, I., Mages, J., Lang, R., Martin, R., Gold, R., Becher, B., Bruck, W., Kalinke, U., 2008. Distinct and nonredundant in vivo functions of IFNAR on myeloid cells limit autoimmunity in the central nervous system. Immunity 28, 675–686.
Rumble, J.M., Huber, A.K., Krishnamoorthy, G., Srinivasan, A., Giles, D.A., Zhang, X., Wang, L., Segal, B.M., 2015. Neutrophil-related factors as biomarkers in EAE and MS. J. Exp. Med. 212, 23–35.
Sahin, E., Haubenwallner, S., Kuttke, M., Kollmann, I., Halfmann, A., Dohnal, A.M., Chen, L., Cheng, P., Hoesel, B., Einwallner, E., Brunner, J., Kral, J.B., Schrottmaier, W.C., Thell, K., Saferding, V., Bluml, S., Schabbauer, G., 2014. Macrophage PTEN regulates expression and secretion of arginase I modulating innate and adaptive immune responses. J. Immunol. Baltimore, Md 1950 (193), 1717–1727.
Sahin, E., Brunner, J.S., Kral, J.B., Kuttke, M., Hanzl, L., Datler, H., Paar, H., Neuwinger, N., Saferding, V., Zinser, E., Halfmann, A., Soukup, K., Hainzl, E., Lohmeyer, T., Niederreiter, B., Haider, T., Dohnal, A.M., Kronke, G., Bluml, S., Schabbauer, G., 2015. Loss of Phosphatase and Tensin Homolog in APCs Impedes Th17-Mediated Autoimmune Encephalomyelitis. J. Immunol. Baltimore, Md 1950 (195), 2560–2570.
Vergadi, E., Ieronymaki, E., Lyroni, K., Vaporidi, K., Tsatsanis, C., 2017. Akt Signaling Pathway in Macrophage Activation and M1/M2 Polarization. J. Immunol. Baltimore, Md 1950 (198), 1006–1014.
Wang, Z., Hong, J., Sun, W., Xu, G., Li, N., Chen, X., Liu, A., Xu, L., Sun, B., Zhang, J.Z., 2006. Role of IFN-gamma in induction of Foxp3 and conversion of CD4+ CD25- T cells to CD4+ Tregs. J. Clin. Invest. 116, 2434–2441.
Willenborg, D.O., Fordham, S., Bernard, C.C., Cowden, W.B., Ramshaw, I.A., 1996. IFN-gamma plays a critical down-regulatory role in the induction and effector phase of myelin oligodendrocyte glycoprotein-induced autoimmune encephalomyelitis. J. Immunol. Baltimore, Md 1950 (157), 3223–3227.
Xue, Z., Li, W., Wang, H., Huang, B., Ge, Z., Gu, C., Liu, Y., Zhang, K., Yang, J., Han, R., Peng, M., Li, Y., Zhang, D., Da, Y., Yao, Z., Zhang, R., 2014. ZSTK474, a novel PI3K inhibitor, modulates human CD14+ monocyte-derived dendritic cell functions and suppresses experimental autoimmune encephalomyelitis. J. Mol. Med. (Berl.) 92, 1057–1068.